

---

# Density Ratio Estimation-based Bayesian Optimization with Semi-Supervised Learning

---

**Jungtaek Kim**

University of Pittsburgh  
jungtaek.kim@pitt.edu

## Abstract

Bayesian optimization has attracted huge attention from diverse research areas in science and engineering, since it is capable of finding a global optimum of an expensive-to-evaluate black-box function efficiently. In general, a probabilistic regression model, e.g., Gaussian processes, random forests, and Bayesian neural networks, is widely used as a surrogate function to model an explicit distribution over function evaluations given an input to estimate and a training dataset. Beyond the probabilistic regression-based Bayesian optimization, density ratio estimation-based Bayesian optimization has been suggested in order to estimate a density ratio of the groups relatively close and relatively far to a global optimum. Developing this line of research further, a supervised classifier can be employed to estimate a class probability for the two groups instead of a density ratio. However, the supervised classifiers used in this strategy tend to be overconfident for a global solution candidate. To solve this overconfidence problem, we propose density ratio estimation-based Bayesian optimization with semi-supervised learning. Finally, we demonstrate the experimental results of our methods and several baseline methods in two distinct scenarios with unlabeled point sampling and a fixed-size pool.

## 1 Introduction

Bayesian optimization [9, 18] has attracted immense attention from various research areas such as hyperparameter optimization [5], battery lifetime optimization [1], and chemical reaction optimization [38], since it is capable of finding a global optimum of an expensive-to-evaluate black-box function in a sample-efficient manner. As studied in previous literature on Bayesian optimization [40, 30, 43, 22], a probabilistic regression model, which can estimate a distribution of function evaluations over inputs, is widely used as a surrogate function; Gaussian process (GP) regression [35] is a predominant choice for the surrogate. An analogy between probabilistic regression models in Bayesian optimization is that they rely on an explicit function over function evaluations  $p(y \mid \mathbf{x}, \mathcal{D})$  given an input we desire to estimate  $\mathbf{x}$  and a training dataset  $\mathcal{D}$ .

Beyond the probabilistic regression-based Bayesian optimization, density ratio estimation (DRE)-based Bayesian optimization has been studied recently [5, 46]. Furthermore, likelihood-free Bayesian optimization, which is equivalent to DRE-based Bayesian optimization with a particular utility function, has been proposed by Song et al. [42]. Bergstra et al. [5] attempt to model two densities  $p(\mathbf{x} \mid y \leq y^\dagger, \mathcal{D})$  and  $p(\mathbf{x} \mid y > y^\dagger, \mathcal{D})$ , where  $y^\dagger$  is a threshold for dividing inputs to two groups that are relatively close and relatively far to a global solution, in order to estimate  $\zeta$ -relative density ratio [49]. On the other hand, instead of modeling two densities separately, Tiao et al. [46], Song et al. [42] estimate a density ratio using class-probability estimation [34]. As discussed in the previous work, this line of research provides a new understanding of Bayesian optimization, which allows us to solve Bayesian optimization using binary classification. Moreover, it can reduce the amount of computations required for building surrogate functions.

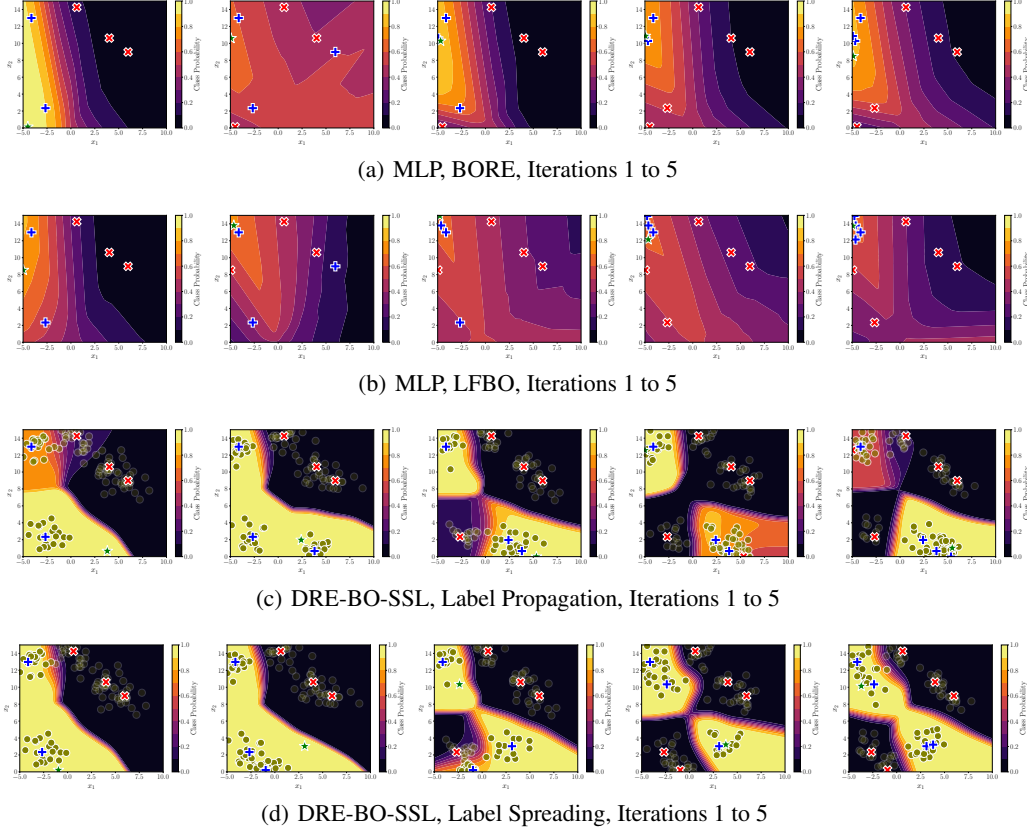


Figure 1: Comparisons of BORE and LFBO by multi-layer perceptrons, and DRE-BO-SSL with label propagation and label spreading for the Branin function. Each row shows Iterations 1 to 5 with five initial points. + (blue), x (red), and \* (green) indicate data points of  $y \leq y^\dagger$ , data points of  $y > y^\dagger$ , and query points, respectively. Moreover, o (olive) stands for unlabeled points and its transparency represents the class probability predicted by a semi-supervised classifier. A query point is chosen by maximizing the output of the classifier. More results are shown in Figures s.1 and s.2.

However, the supervised classifier utilized in the DRE-based Bayesian optimization tends to be overconfident for a global solution candidate (or a potential region that exists a global solution). In this paper, to solve this overconfidence problem, we propose a novel DRE-based method with semi-supervised learning, named DRE-BO-SSL. Although our unequivocal competitors, i.e., BORE [46] and LFBO [42], show their strengths through theoretical and empirical analyses, our algorithm better an ability to consider a wider region that satisfies  $p(\mathbf{x} \mid y \leq y^\dagger, \mathcal{D}) \geq p(\mathbf{x} \mid y > y^\dagger, \mathcal{D})$ , than the competitors, as shown in Figure 1. By this intuitive example in Figure 1, we presume that DRE-BO-SSL appropriately balances exploration and exploitation rather than the existing methods. Compared to a supervised classifier, e.g., random forests [8], gradient boosting [16], and multi-layer perceptrons, our semi-supervised classifiers, i.e., label propagation [53] and label spreading [51], are less confident in terms of the regions of global solution candidates by utilizing unlabeled data points; see Figures 1, s.1, and s.2 and Section 3 for detailed examples and analyses.

To make use of semi-supervised classifiers, we take into account two distinct scenarios with unlabeled point sampling and with a predefined fixed-size pool. For the first scenario, we randomly sample unlabeled data points from the truncated multivariate normal distribution using a minimax tilting method [7], in order that a cluster assumption [37] is assumed. Finally, we show that our method outperforms the exiting methods in diverse experiments including synthetic benchmark functions, Tabular Benchmarks [26], NATS-Bench [15], and minimum multi-digit MNIST search.

To sum up, our contributions are itemized as follows: (i) we identify the overconfidence problem of supervised classifiers in DRE-based Bayesian optimization; (ii) we propose DRE-based Bayesian optimization with semi-supervised learning, named DRE-BO-SSL for two distinct scenarios with

unlabeled point sampling and a predefined fixed-size pool; (iii) we demonstrate the effectiveness of our method in various experiments including NATS-Bench and minimum multi-digit MNIST search.

*We promise to release our implementation upon publication.*

## 2 Background and Related Work

**Bayesian Optimization.** It is a principled and efficient approach to finding a global solution of a challenging objective, e.g., expensive-to-evaluate black-box functions [9, 18]. In this paragraph, to focus on a probabilistic regression model as a surrogate function, we omit the details of Bayesian optimization; see [9, 18] for its details. In the Bayesian optimization community, GP regression [35] is widely used as a surrogate function [44, 40] because of its flexibility with minimum assumptions on model and smoothness. While GP is a probable choice, Bayesian optimization with diverse surrogate functions such as Student- $t$  process regression [30], Bayesian neural networks [43], and tree-based models [22, 24] has been proposed. An analogy between such models is that they model  $p(y | \mathbf{x}, \mathcal{D})$  explicitly, so that it can be used to define an acquisition function with the statistics of  $p(y | \mathbf{x}, \mathcal{D})$ .

**Density-Ratio Estimation.** Whereas knowing a data distribution  $p(\mathbf{x})$  is important, it is difficult to directly estimate  $p(\mathbf{x})$  [45]. For particular machine learning problems such as importance sampling [27] and mutual information estimation [6], we can bypass direct density estimation and estimate a density ratio. In Bayesian optimization, Bergstra et al. [5] propose a strategy with tree-structured Parzen estimators to estimate a density ratio as an alternative to probabilistic regression-based acquisition functions. In addition, the work [46, 42] suggests a method with binary classifiers in order to estimate class probabilities as a density ratio; see Section 3 for their details.

**Semi-Supervised Learning.** It is a learning scheme with both labeled and unlabeled data [52, 12, 4]. To cooperate with labeled and unlabeled data, this strategy generally utilizes geometry of data points or connectivity between points, and assigns a pseudo-label to unlabeled data, which referred to as transductive learning [17]. As a semi-supervised learning method on a similarity graph, Zhu and Ghahramani [53] propose a label propagation algorithm which iteratively propagates the labels of unlabeled data points using labeled data. Zhou et al. [51] compute the labels of labeled and unlabeled data points by a weighted iterative algorithm with initial labels. Belkin and Niyogi [2] predict pseudo-labels by finding a linear combination of a few smallest eigenvectors of the graph Laplacian.

## 3 DRE-based Bayesian Optimization

Unlike probabilistic regression-based Bayesian optimization, DRE-based Bayesian optimization employs a density ratio-based acquisition function, which is defined with a density  $p(\mathbf{x} | y \leq y^\dagger, \mathcal{D}_t)$ , where  $\mathbf{x}$  is a  $d$ -dimensional vector,  $y$  is its function evaluation,  $y^\dagger$  is a threshold, and  $\mathcal{D}_t = \{(\mathbf{x}_i, y_i)\}_{i=0}^t$  is a dataset of  $t + 1$  pairs of data point and evaluation. In particular, the work by Bergstra et al. [5] defines an acquisition function based on  $\zeta$ -relative density ratio [49]:

$$A(\mathbf{x} | \zeta, \mathcal{D}_t) = \frac{p(\mathbf{x} | y \leq y^\dagger, \mathcal{D}_t)}{\zeta p(\mathbf{x} | y \leq y^\dagger, \mathcal{D}_t) + (1 - \zeta)p(\mathbf{x} | y > y^\dagger, \mathcal{D}_t)}, \quad (1)$$

where  $\zeta = p(y \leq y^\dagger) \in [0, 1)$  is a threshold ratio. We need to find a maximizer of (1), by optimizing the following composite function:  $h(p(\mathbf{x} | y \leq y^\dagger, \mathcal{D}_t)/p(\mathbf{x} | y > y^\dagger, \mathcal{D}_t))$ , from (1) where  $h(x) = (\zeta + (1 - \zeta)x^{-1})^{-1}$ . Since  $h$  is a strictly increasing function, we can directly maximize  $p(\mathbf{x} | y \leq y^\dagger, \mathcal{D}_t)/p(\mathbf{x} | y > y^\dagger, \mathcal{D}_t)$ . In the previous work [5], two tree-structured Parzen estimators are used to estimate the respective densities,  $p(\mathbf{x} | y \leq y^\dagger, \mathcal{D}_t)$  and  $p(\mathbf{x} | y > y^\dagger, \mathcal{D}_t)$ .

While the work [5] utilizes two distinct tree-structured Parzen estimators, Tiao et al. [46] propose a method to directly estimate (1) using class-probability estimation [34, 45], called BORE. Since it can be formulated as a problem of binary classification in which class 1 is a group of top  $\zeta$  of  $\mathcal{D}_t$  and class 0 is a group of bottom  $1 - \zeta$  of  $\mathcal{D}_t$ , the acquisition function defined in (1) induces the following:

$$A(\mathbf{x} | \zeta, \mathcal{D}_t) = \frac{p(\mathbf{x} | z = 1)}{\zeta p(\mathbf{x} | z = 1) + (1 - \zeta)p(\mathbf{x} | z = 0)}. \quad (2)$$

By the Bayes' theorem, (2) becomes  $A(\mathbf{x} \mid \zeta, \mathcal{D}_t) = \zeta^{-1}p(z = 1 \mid \mathbf{x})/(p(z = 1 \mid \mathbf{x}) + p(z = 0 \mid \mathbf{x}))$ . Therefore, a class probability over  $\mathbf{x}$  for class 1 is considered as an acquisition function; it is simply denoted as  $A(\mathbf{x} \mid \zeta, \mathcal{D}_t) = \zeta^{-1}\pi(\mathbf{x})$ . Eventually, the class probability is estimated by various off-the-shelf classifiers such as random forests and multi-layer perceptrons.

Song et al. [42] suggest a general framework of likelihood-free Bayesian optimization, called LFBO:

$$A(\mathbf{x} \mid \zeta, \mathcal{D}_t) = \arg \max_{S: \mathcal{X} \rightarrow \mathbb{R}} \mathbb{E}_{\mathcal{D}_t} [u(y; y^\dagger) f'(S(\mathbf{x})) - f^*(f'(S(\mathbf{x})))], \quad (3)$$

which is versatile for any non-negative utility function  $u(y; y^\dagger)$ , where  $f$  is a strictly convex function and  $f^*$  is the convex conjugate of  $f$ . By the properties of LFBO, it is equivalent to an expected utility-based acquisition function. Along with the general framework, Song et al. [42] prove that BORE is equivalent to the probability of improvement [28] and LFBO with  $u(y; y^\dagger) = \mathbb{I}(y \leq y^\dagger)$  is also equivalent to the probability of improvement, where  $\mathbb{I}$  is an indicator function. Moreover, they show that their method with  $u(y; y^\dagger) = \max(y^\dagger - y, 0)$ , which can be implemented as weighted binary classification, is equivalent to the expected improvement [31].

### 3.1 Overconfidence Problem

As mentioned in Section 1 and shown in Figures 1, s.1, and s.2, the supervised classifiers used in DRE-based Bayesian optimization suffer from the overconfidence problem. Interestingly, many deep learning models also share a similar overconfidence problem [20, 32], due to various reasons, but primarily due to overparameterization.

However, the definition of the overconfidence problem in DRE-based Bayesian optimization is slightly different from one in general classification. The definition in DRE-based Bayesian optimization does not imply that a single data point has a high probability for a particular class, but it implies that a few data points have high probabilities for a class of interest. More precisely, our definition indicates a problem of overconfidence over global solution candidates. For example, the definition in general classification includes a case that 50% of data points are biased to one class and the remainder is biased to another class. On the contrary, our definition does not include such a case and it only includes a case that a small number of data points are biased to some class, i.e., class 1 in our problem.

By the aforementioned definition, at early iterations of Bayesian optimization, a supervised classifier tends to overfit to a small size of  $\mathcal{D}_t$  due to a relatively large model capacity. This consequence makes a Bayesian optimization algorithm highly focus on exploitation. It is also different from the aspect of probabilistic regression-based Bayesian optimization because the regression-based Bayesian optimization is capable of exploring unseen regions by dealing with uncertainties. Besides, even though a threshold  $\zeta$  might be able to mitigate this problem, an overconfident supervised classifier is likely to keep getting stuck in a local optimum since  $y^\dagger$  cannot change dramatically.

## 4 DRE-based Bayesian Optimization with Semi-Supervised Learning

We introduce DRE-based Bayesian optimization with semi-supervised learning, named DRE-BO-SSL, by following previous studies in DRE-based and likelihood-free Bayesian optimization [5, 46, 42], which were discussed in Section 3.

Similar to the standard Bayesian optimization and existing DRE-based Bayesian optimization, DRE-BO-SSL iterates the undermentioned steps as presented in Algorithm 1. First, a threshold  $y_t^\dagger$  is computed by considering  $y_{1:t}$  with  $\zeta$ . Second, labels  $\mathbf{C}_t$  of data points in  $\mathcal{D}_t$  are assigned to one of two classes; a group of  $y \leq y_t^\dagger$  is assigned to Class 1 and a group of  $y > y_t^\dagger$  is assigned to Class 0. If we are given unlabeled data points  $\mathbf{X}_u$ , the corresponding points  $\mathbf{X}_u$  are used, but if not available it samples  $n_u$  unlabeled data points  $\mathbf{X}_u$  from  $\mathcal{X}$  by utilizing a strategy described in Section 4.2. Then, it estimates pseudo-labels  $\hat{\mathbf{C}}_t$  of a semi-supervised learning model by following the procedure in Section 4.1 and Algorithm s.1. Using  $\hat{\mathbf{C}}_t$ , it chooses the next query point  $\mathbf{x}_{t+1}$ :

$$\mathbf{x}_{t+1} = \arg \max_{\mathbf{x} \in \mathcal{X}} \pi_{\hat{\mathbf{C}}_t}(\mathbf{x}; \zeta, \mathcal{D}_t, \mathbf{X}_u), \quad (4)$$

where  $\pi_{\hat{\mathbf{C}}_t}(\mathbf{x}; \zeta, \mathcal{D}_t, \mathbf{X}_u)$  predicts a class probability over  $\mathbf{x}$  for Class 1; see (8).

---

**Algorithm 1** DRE-BO-SSL

---

**Input:** Iteration budget  $T$ , a search space  $\mathcal{X}$ , a black-box objective  $f$ , a threshold ratio  $\zeta$ , a semi-supervised classifier  $\pi_{\mathbf{C}}$ , and unlabeled data points  $\mathbf{X}_u$  if available and the number of unlabeled data points  $n_u$ , otherwise.

**Output:** Best candidate  $\mathbf{x}^+$ .

- 1: Initialize  $\mathcal{D}_0 = \{(\mathbf{x}_0, y_0)\}$  by randomly selecting  $\mathbf{x}_0$  from  $\mathcal{X}$  and evaluating  $\mathbf{x}_0$  by  $f$ .
  - 2: **for**  $t = 0$  **to**  $T - 1$  **do**
  - 3:   Compute a threshold  $y_t^\dagger$  using  $\zeta$ .
  - 4:   Assign labels  $\mathbf{C}_t$  of data points in  $\mathcal{D}_t$  with  $y_t^\dagger$ .
  - 5:   **if**  $\mathbf{X}_u$  are not available **then**
  - 6:     Sample  $n_u$  unlabeled data points  $\mathbf{X}_u$  from  $\mathcal{X}$ .
  - 7:   **end if**
  - 8:   Estimate pseudo-labels  $\hat{\mathbf{C}}_t$  by following the procedure in Algorithm s.1.
  - 9:   Choose the next query point  $\mathbf{x}_{t+1}$  by maximizing  $\pi_{\hat{\mathbf{C}}_t}(\mathbf{x}; \zeta, \mathcal{D}_t, \mathbf{X}_u)$  for  $\mathbf{x} \in \mathcal{X}$ .
  - 10:   Evaluate  $\mathbf{x}_{t+1}$  by  $f$  and update  $\mathcal{D}_{t+1}$ .
  - 11: **end for**
  - 12: Determine the best candidate  $\mathbf{x}^+$ , considering  $y_{0:T}$ .
- 

We adopt a multi-started local optimization technique, e.g., L-BFGS-B [10], to solve (4). However, a flat landscape of  $\pi_{\hat{\mathbf{C}}_t}(\mathbf{x}; \zeta, \mathcal{D}_t, \mathbf{X}_u)$  over  $\mathbf{x}$  may occur, so that optimization performance can be degraded. To solve this issue, a simple heuristic of randomly selecting a query point among points with identical highest class probabilities complements our method. Since the multi-started technique is utilized and the output of  $\pi_{\hat{\mathbf{C}}_t}$  is bounded in  $[0, 1]$ , a flat landscape is easily recognized by comparing the outcomes of the multi-started strategy. See the detailed discussion on this issue in Section 6.

#### 4.1 Label Propagation and Label Spreading

Here we describe semi-supervised learning techniques [52, 12, 4] to build DRE-BO-SSL. We cover a transductive setting [17], which is to label unlabeled data by utilizing given labeled data, and then an inductive setting, which is to predict any point using pseudo-labels of unlabeled and labeled data.

Suppose that each data point is defined on a  $d$ -dimensional compact space  $\mathcal{X} \subset \mathbb{R}^d$ . We consider  $n_l$  labeled points  $\mathbf{X}_l \in \mathbb{R}^{n_l \times d}$ , their corresponding labels  $\mathbf{C}_l \in \mathbb{R}^{n_l \times c}$ , and  $n_u$  unlabeled points  $\mathbf{X}_u \in \mathbb{R}^{n_u \times d}$ , where  $c$  is the number of classes.  $\mathbf{X}_l$  and  $\mathbf{C}_l$  are query points that have already been evaluated and their class labels; we define  $\mathbf{X}_l = [\mathbf{x}_0, \dots, \mathbf{x}_{n_l-1}]^\top$  for  $\mathcal{D}_t = \{(\mathbf{x}_i, y_i)\}_{i=0}^{n_l-1}$ . For the sake of brevity, the concatenated data points of  $\mathbf{X}_l$  and  $\mathbf{X}_u$  are defined as  $\mathbf{X} = [\mathbf{X}_l; \mathbf{X}_u] \in \mathbb{R}^{(n_l+n_u) \times d}$ . In our problem,  $c = 2$  because we solve density-ratio estimation with two classes, i.e., 0 and 1.

As shown in Algorithm s.1, we first initialize labels to propagate  $\hat{\mathbf{C}} \in \mathbb{R}^{(n_l+n_u) \times 2}$ ; it is initialized as  $\hat{\mathbf{C}} = [\mathbf{c}_0, \dots, \mathbf{c}_{n_l-1}, \mathbf{c}_{n_l}, \dots, \mathbf{c}_{n_l+n_u-1}]^\top$ , where  $\mathbf{c}_0, \dots, \mathbf{c}_{n_l-1}$  are one-hot representations  $[\mathbf{C}_l]_i$  for  $i \in [n_l]$  and  $\mathbf{c}_{n_l}, \dots, \mathbf{c}_{n_l+n_u-1}$  are zero vectors. Then, we need to compute a similarity between two data points  $\mathbf{x}_i, \mathbf{x}_j \in \mathcal{X}$ , so that we compare all pairs in  $\mathbf{X}$ . For example, one of popular similarity functions, i.e., a radial basis function kernel, is the following:

$$w_{ij} = \exp(-\beta \|\mathbf{x}_i - \mathbf{x}_j\|_2^2), \quad (5)$$

where  $\beta$  is a free parameter given. As discussed in the work [53], we can learn  $\beta$  in (5) by minimizing an entropy for propagated labels  $\hat{\mathbf{C}}$ :  $H = -\sum_{i=1}^{n_l+n_u} [\hat{\mathbf{C}}]_i^\top \log[\hat{\mathbf{C}}]_i$ ; see Section S.4 for analysis on the effects of  $\beta$ . By (5), we compute a transition probability from  $\mathbf{x}_j$  to  $\mathbf{x}_i$  by  $p_{ij} = w_{ij} / \sum_{k=1}^{n_l+n_u} w_{kj}$ . Note that similarities  $\mathbf{W} \in \mathbb{R}^{(n_l+n_u) \times (n_l+n_u)}$  and transition probabilities  $\mathbf{P} \in \mathbb{R}^{(n_l+n_u) \times (n_l+n_u)}$  are defined, where  $[\mathbf{W}]_{ij} = w_{ij}$  and  $[\mathbf{P}]_{ij} = p_{ij}$ . Moreover, by the definition of  $p_{ij}$ ,  $\mathbf{P} = \mathbf{D}^{-1} \mathbf{W}$ , where  $\mathbf{D}$  is a degree matrix whose diagonal entry is defined as  $[\mathbf{D}]_{ii} = \sum_{j=1}^{n_l+n_u} [\mathbf{W}]_{ij}$ .

With initial  $\hat{\mathbf{C}}$  and  $\mathbf{P}$ , we repeat the following steps: (i) computing the next  $\hat{\mathbf{C}}$ ; (ii) normalizing  $\hat{\mathbf{C}}$  row-wise, until a change of  $\hat{\mathbf{C}}$  converges to a tolerance  $\varepsilon$  or the number of iterations propagated reaches to maximum iterations  $\tau$ . In particular, label propagation [53] updates  $\hat{\mathbf{C}}$  and constrains the labels of labeled data to  $\mathbf{C}_l$ :

$$\hat{\mathbf{C}}_{t+1} \leftarrow \mathbf{P}^\top \hat{\mathbf{C}}_t \quad \text{and} \quad [\hat{\mathbf{C}}_{t+1}]_i \leftarrow [\mathbf{C}_l]_i, \quad (6)$$

for  $i \in [n_l]$  at Iteration  $t$ . On the other hand, label spreading [51] propagates  $\hat{\mathbf{C}}$  by allowing a change of the labels of labeled data with a clamping factor  $\alpha \in (0, 1)$ :

$$\hat{\mathbf{C}}_{t+1} \leftarrow \alpha \mathbf{D}^{-1/2} \mathbf{W} \mathbf{D}^{-1/2} \hat{\mathbf{C}}_t + (1 - \alpha) \hat{\mathbf{C}}_0, \quad (7)$$

where  $\hat{\mathbf{C}}_0$  is the initial propagated labels defined Line 1 of Algorithm s.1. Note that  $\mathbf{D}^{-1/2} \mathbf{W} \mathbf{D}^{-1/2}$  can be pre-computed before the loop defined from Line 4 to Line 7.

By the nature of transductive setting, it only predicts the labels of particular data using particular known data [17], which implies that it cannot estimate a categorical distribution of unseen data. To enable it, given unseen data point  $\mathbf{x}$ , we define an inductive model with  $\hat{\mathbf{C}}$ :

$$\hat{c}_i = \frac{\mathbf{w}^\top [\hat{\mathbf{C}}]_{:i}}{\sum_{j=1}^c \mathbf{w}^\top [\hat{\mathbf{C}}]_{:j}}, \quad (8)$$

for  $i \in [2]$ , where  $\mathbf{w} \in \mathbb{R}^{n_l+n_u}$  is similarities of  $\mathbf{x}$  and  $\mathbf{X}$  by (5). This inductive model is better than or equivalent to other classifiers without unlabeled data; its analysis will be provided in Section 4.3.

## 4.2 Unlabeled Point Sampling

As described above, if unlabeled points are not available, we need to generate unlabeled points under a transductive learning scheme. However, it is a challenging problem unless we know a landscape of  $\pi_{\mathbf{C}}$  adequately. Many studies [37, 36, 39, 3, 11, 48, 50] investigate how unlabeled data can affect a model and whether unlabeled data helps to improve the model or not.

To enjoy the theoretical findings of previous literature, we define a cluster assumption:

**Assumption 4.1** (Cluster assumption in [37]). *Two points  $\mathbf{x}_i, \mathbf{x}_j \in \mathcal{X}$  should belong to the same label if there is a path between  $\mathbf{x}_i$  and  $\mathbf{x}_j$  which passes only through regions of relatively high  $P(X)$ , where  $P$  is a distribution over a random variable  $X \in \mathcal{X}$ .*

By Assumption 4.1, the idea of clustering on the Euclidean space or spectral clustering on a graph can be naturally applied in semi-supervised learning [37, 23], which is not the scope of this work.

To build DRE-BO-SSL associated with Assumption 4.1, we sample unlabeled data points from the truncated multivariate normal distribution so that each sample is in a compact  $\mathcal{X}$ :

$$f(\mathbf{z}) = \frac{\exp(-\frac{1}{2} \mathbf{z}^\top \mathbf{z}) \mathbb{I}(\mathbf{l} \leq \mathbf{A} \mathbf{z} \leq \mathbf{u})}{P(\mathbf{l} \leq \mathbf{A} \mathbf{Z} \leq \mathbf{u})}, \quad (9)$$

where  $\mathbf{l}, \mathbf{u} \in \mathbb{R}^d$  are lower and upper bounds,  $\mathbf{\Sigma} = \mathbf{A} \mathbf{A}^\top$  is a covariance matrix,  $\mathbb{I}$  is an indicator function, and  $\mathbf{Z} \sim \mathcal{N}(\mathbf{0}, \mathbf{I}_d)$  is a random variable. It is challenging to compute a denominator of (9),  $P(\mathbf{l} \leq \mathbf{A}^\top \mathbf{Z} \leq \mathbf{u})$ , and simulate from  $f(\mathbf{z})$  because an integration of the denominator and an accept-reject sampling strategy from  $f(\mathbf{z})$  are cumbersome in this multi-dimensional case. To effectively sample from the truncated multivariate normal distribution, we adopt a minimax tilting method [7]. Compared to a method by Genz [19], it yields a high acceptance rate and accurate sampling. We will provide more thorough discussion on point sampling in Sections 6 and S.5.

## 4.3 Analysis

Under the cluster assumption, i.e., Assumption 4.1, a margin  $\gamma$  is defined as a minimum distance between two decision boundaries.

**Definition 4.2.** *Let a compact connected decision set be  $\mathcal{C}_i \subseteq \mathcal{X}$  for  $i \in \{0, 1\}$  and a boundary subset, i.e., a set of boundary points, of a compact connected set  $\mathcal{S}$  be  $\partial \mathcal{S}$ . A margin  $\gamma$  is defined as*

$$\gamma = (2\mathbb{I}(\mathcal{C}_1 \cap \mathcal{C}_2 = \emptyset) - 1) \min_{\mathbf{x}_1 \in \partial \mathcal{C}_1 \setminus \partial \mathcal{X}, \mathbf{x}_2 \in \partial \mathcal{C}_2 \setminus \partial \mathcal{X}} \|\mathbf{x}_1 - \mathbf{x}_2\|_2. \quad (10)$$

Using Definition 4.2, we claim that a semi-supervised classifier in DRE-BO-SSL can mitigate the overconfidence problem presented in Section 3.1, because it can expand a decision set  $\mathcal{C}_1$  for class 1 by reducing  $\gamma$  with unlabeled data. However, we need to verify if a large decision set is derived from the characteristics of non-parametric classifiers, since a semi-supervised classifier we use is

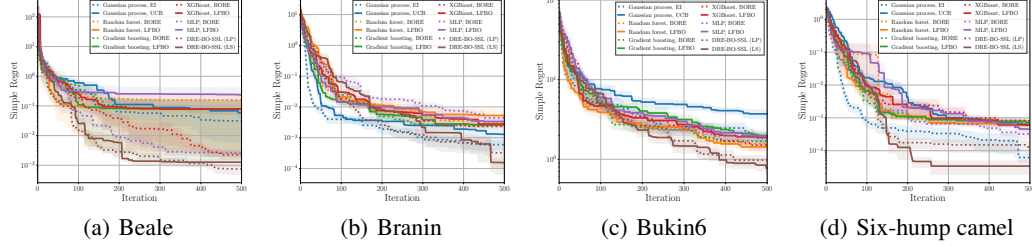


Figure 2: Results of synthetic benchmark functions for a scenario with unlabeled point sampling. All experiments are repeated 10 times. LP and LS stand for label propagation and label spreading.

converted to the Nadaraya-Watson non-parametric model [33, 47] without unlabeled data. As shown in Figure S.5, a semi-supervised classifier without unlabeled data, i.e., the Nadaraya-Watson estimator, does not perform well compared to the classifiers with unlabeled data. It implies that the presence of unlabeled data is effective for alleviating the overconfidence problem.

Singh et al. [39] provide a sample error bound of supervised and semi-supervised learners, related to  $\gamma$ ,  $n_l$ ,  $n_u$ , and  $d$ . Suppose that an error is  $\mathcal{E}(\hat{f}) = \mathcal{R}(\hat{f}) - \mathcal{R}^*$  where  $\mathcal{R}$  is a risk and  $\mathcal{R}^*$  is the infimum risk over all learners. The lower bound of finite sample error for any supervised learners is

$$\inf_{f_i} \sup_{P_{XY}(\gamma)} \mathbb{E}[\mathcal{E}(f_i)] \geq \epsilon_1(n_l). \quad (11)$$

By Corollary 1 in [39], supposing that there exists a perfect supervised learner  $\hat{f}_{\mathcal{C}, n_l}$ :

$$\sup_{P_{XY}(\gamma)} \mathbb{E}[\mathcal{E}(\hat{f}_{\mathcal{C}, n_l})] \leq \epsilon_2(n_l), \quad (12)$$

with perfect knowledge of decision sets  $\mathcal{C}$ . Then, there exists a semi-supervised learner  $\hat{f}_{n_l, n_u}$ :

$$\sup_{P_{XY}(\gamma)} \mathbb{E}[\mathcal{E}(\hat{f}_{n_l, n_u})] \leq \epsilon_2(n_l) + g(n_l, n_u, d) \approx \epsilon_2(n_l), \quad (13)$$

if  $n_u \gg n_l$ . Thus, by borrowing the theoretical results of the work [39], we can conclude that  $\epsilon_2(n_l) < \epsilon_1(n_l)$  can be satisfied, which implies that a semi-supervised learner can be better than any supervised learners, by assuming that  $n_u \gg n_l$  and access to perfect knowledge of decision sets. Consequently, we can claim that our proposed method DRE-BO-SSL is able to be better than an approach with supervised classifiers in our problem formulation.

## 5 Experiments

We test DRE-BO-SSL and baseline methods in the following circumstances: synthetic benchmarks for a scenario with unlabeled point sampling, and synthetic benchmarks, Tabular Benchmarks [26], NATS-Bench [15], and minimum multi-digit MNIST search for a scenario with a fixed-size pool. Note that Tabular Benchmarks, NATS-Bench, and minimum multi-digit MNIST search are defined with a fixed number of possible solution candidates, which implies that they are considered as combinatorial optimization problems. By following the previous work [46, 42], we set a threshold ratio as  $\zeta = 0.33$  for all experiments. To solve (4), we use L-BFGS-B [10] with 1000 different initializations. All experiments are repeated 10 times with 10 fixed random seeds. Other missing details including the details of the competitors of our methods are presented in Section S.3.

### 5.1 A Scenario with Unlabeled Point Sampling

**Synthetic Benchmarks.** We run several synthetic functions for our methods and the baseline methods. For unlabeled point sampling, we sample 100 points from  $\mathcal{N}(\mathbf{x}_1, \mathbf{I}_d), \dots, \mathcal{N}(\mathbf{x}_{n_l}, \mathbf{I}_d)$ , where  $\lfloor n_u/n_l \rfloor$  or  $\lfloor n_u/n_l \rfloor + 1$  points are sampled from each truncated distribution, so that  $n_u$  points are sampled in total. Our methods outperform the baseline methods, as shown in Figure 2.

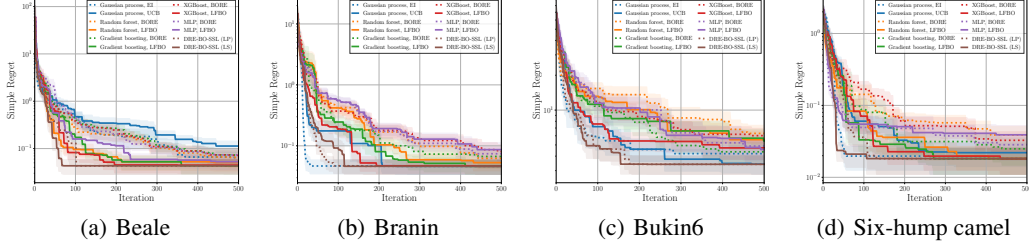


Figure 3: Results of synthetic benchmark functions for a scenario with fixed-size pools. All experiments are repeated 10 times. LP and LS stand for label propagation and label spreading.

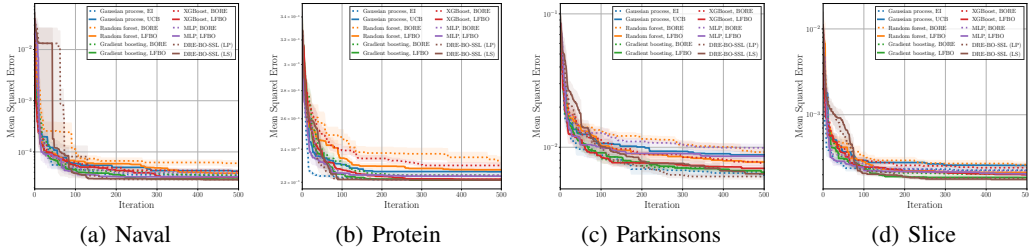


Figure 4: Results of Tabular Benchmarks for a scenario with fixed-size pools. All experiments are repeated 10 times. LP and LS stand for label propagation and label spreading.

## 5.2 Scenarios with Fixed-Size Pools

**Synthetic Benchmarks.** Several synthetic benchmark functions are tested for our methods and the baseline methods. To generate a fixed-size pool for each benchmark, we uniformly sample 1000 points from a bounded search space before an optimization round is started. As presented in Figure 3, our methods perform better than the baseline methods.

**Tabular Benchmarks.** The comparisons of our methods and the existing methods are carried out in these hyperparameter optimization benchmarks [26]. We can benchmark a variety of machine learning models, which are trained on four datasets: naval propulsion, protein structure, parkinsons telemonitoring, and slice localization. There exist 62,208 models, which are used as a pool, for each dataset. Our methods show the superior performance compared to the other approaches.

**NATS-Bench.** NATS-Bench [15], which is the up-to-date version of NAS-Bench-201 [14], is used to test our methods and the baseline methods. NATS-Bench is a neural architecture search benchmark with three popular datasets: CIFAR-10, CIFAR-100, and ImageNet-16-120, and it has 32,768 architectures, i.e., a fixed-size pool, for each dataset. Our methods work well in three datasets, compared to the existing methods. The details can be found in Section S.3.

**Minimum Multi-Digit MNIST Search.** This task, which is proposed in this work, is to find a minimum multi-digit number, where a fixed number of multi-digit MNIST images are given. As visualized in Figure 5, three random images in the MNIST dataset [29] are concatenated. Eventually, “000” are global minimum and “999” are global maximum, respectively. Since inputs are images and each concatenated image consists of three different digit images, this optimization problem is challenging. The size of a fixed-size pool is 80,000. As shown in Figure 5, our method outperforms other baselines.

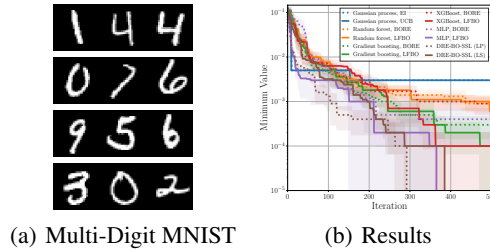


Figure 5: Minimum multi-digit MNIST search.

Missing details of all the experiments are described in Section S.3 of the supplementary material.



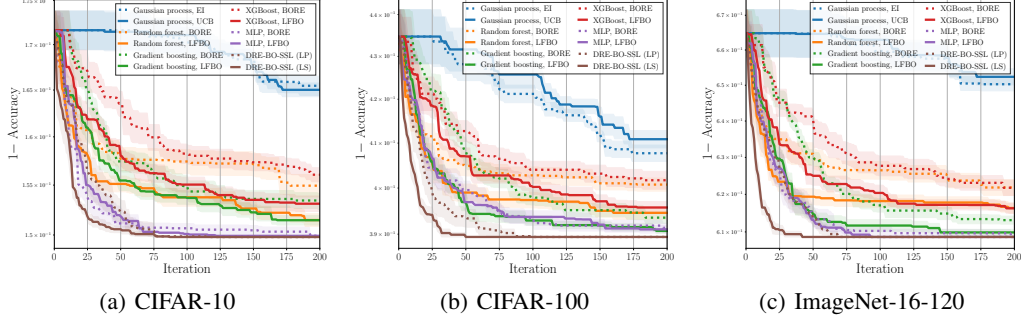


Figure 6: Results of NATS-Bench for a scenario with fixed-size pools. All experiments are repeated 10 times. LP and LS stand for label propagation and label spreading.

## 6 Discussion

We discuss important topics on our methods and the properties of DRE-BO-SSL. Moreover, we include more thorough discussion and broader impacts in the supplementary material.

**Flat Landscape of Class Probabilities over Inputs.** Regardless of use of either supervised or semi-supervised classifier, a flat landscape of class probabilities can occur in the framework of DRE-based Bayesian optimization. To overcome the issue of optimizing a flat landscape, we add a simple heuristic of selecting a random query point from points with identical highest class probabilities if the landscape is flat, as described in Section 4. Since off-the-shelf local optimization methods struggle for optimizing a flat landscape, this simple heuristic is effective.

**Effects of Sampling Distributions for Unlabeled Points.** We choose a distribution for unlabeled point sampling as the truncated multivariate normal distribution in order to satisfy the cluster assumption. Beyond the normal distribution, we demonstrate the effects of sampling distributions for unlabeled points in Section S.5 of the supplementary material, utilizing diverse sampling distributions, i.e., uniform distributions, Halton sequences [21], and Sobol’ sequences [41].

**Effects of Pool Sampling.** Since the computational complexity of label propagation and label spreading depends on a pool size, we need to reduce a pool size appropriately in order to speed up the algorithms. Therefore, we uniformly sample a subset of the fixed-size set, which is employed as unlabeled points. Analysis on the effects of pool sampling is demonstrated in Section S.6.

**General Framework of DRE-BO-SSL.** As a future research direction, we expect that a general framework of DRE-BO-SSL can be defined, similar to a likelihood-free approach by Song et al. [42]. However, it is difficult to define an utility function involved in both labeled and unlabeled data. For example, if we assume that an utility is  $u(y; y^\dagger) = \max(y^\dagger - y, 0)$ ,  $y$  for unlabeled data point is unknown. Although it depends on the form of utility function, we need to define  $y$  of unlabeled data point by utilizing the information we have if the utility function is related to  $y$ .

**Limitations.** As discussed above, our algorithms slow down if a pool size is significantly large. To solve this issue, we suggest a method to randomly select a subset of the pool, but a more sophisticated subsampling method can be devised for our framework. In particular, we can leverage the impacts of the subset of the pool by utilizing the geometric information of unlabeled data points.

## 7 Conclusion

In this paper we have proposed a DRE-based Bayesian optimization framework with semi-supervised learning, named DRE-BO-SSL. Unlike the existing work such as BORE and LFBO, our methods utilize a semi-supervised classifier, i.e., label propagation and label spreading, where unlabeled data points are sampled or given. The superior results by our methods show the validity of our algorithms. To understand them properly, we provided the elaborate analyses on the properties of DRE-BO-SSL.

## Acknowledgments and Disclosure of Funding

This research was supported in part by the University of Pittsburgh Center for Research Computing through the resources provided. Specifically, this work used the H2P cluster, which is supported by NSF award number OAC-2117681.

## References

- [1] P. M. Attia, A. Grover, N. Jin, K. A. Severson, T. M. Markov, Y.-H. Liao, M. H. Chen, B. Cheong, N. Perkins, Z. Yang, P. K. Herring, M. Aykol, S. J. Harris, R. D. Braatz, S. Ermon, and W. C. Chueh. Closed-loop optimization of fast-charging protocols for batteries with machine learning. *Nature*, 578(7795):397–402, 2020.
- [2] M. Belkin and P. Niyogi. Using manifold structure for partially labeled classification. In *Advances in Neural Information Processing Systems (NeurIPS)*, volume 15, Vancouver, British Columbia, Canada, 2002.
- [3] S. Ben-David, T. Lu, and D. Pál. Does unlabeled data provably help? worst-case analysis of the sample complexity of semi-supervised learning. In *Proceedings of the Annual Conference on Learning Theory (COLT)*, pages 33–44, 2008.
- [4] Y. Bengio, O. Delalleau, and N. Le Roux. Label propagation and quadratic criterion. In O. Chapelle, B. Schölkopf, and A. Zien, editors, *Semi-Supervised Learning*, pages 193–216. MIT Press, 2006.
- [5] J. Bergstra, R. Bardenet, Y. Bengio, and B. Kégl. Algorithms for hyper-parameter optimization. In *Advances in Neural Information Processing Systems (NeurIPS)*, volume 24, pages 2546–2554, Granada, Spain, 2011.
- [6] C. M. Bishop. *Pattern Recognition and Machine Learning*. Springer, 2006.
- [7] Z. I. Botev. The normal law under linear restrictions: simulation and estimation via minimax tilting. *Journal of the Royal Statistical Society B*, 79(1):125–148, 2017.
- [8] L. Breiman. Random forests. *Machine Learning*, 45(1):5–32, 2001.
- [9] E. Brochu, V. M. Cora, and N. de Freitas. A tutorial on Bayesian optimization of expensive cost functions, with application to active user modeling and hierarchical reinforcement learning. *arXiv preprint arXiv:1012.2599*, 2010.
- [10] R. H. Byrd, P. Lu, J. Nocedal, and C. Zhu. A limited memory algorithm for bound constrained optimization. *SIAM Journal on Scientific Computing*, 16(5):1190–1208, 1995.
- [11] Y. Carmon, A. Raghunathan, L. Schmidt, J. C. Duchi, and P. S. Liang. Unlabeled data improves adversarial robustness. In *Advances in Neural Information Processing Systems (NeurIPS)*, volume 32, pages 11192–11203, Vancouver, British Columbia, Canada, 2019.
- [12] O. Chapelle, B. Schölkopf, and A. Zien. *Semi-Supervised Learning*. MIT Press, 2006.
- [13] T. Chen and C. Guestrin. XGBoost: A scalable tree boosting system. In *Proceedings of the ACM SIGKDD Conference on Knowledge Discovery and Data Mining (KDD)*, pages 785–794, San Francisco, California, USA, 2016.
- [14] X. Dong and Y. Yang. NAS-Bench-201: Extending the scope of reproducible neural architecture search. In *Proceedings of the International Conference on Learning Representations (ICLR)*, New Orleans, Louisiana, USA, 2019.
- [15] X. Dong, L. Liu, K. Musial, and B. Gabrys. NATS-Bench: Benchmarking NAS algorithms for architecture topology and size. *IEEE Transactions on Pattern Analysis and Machine Intelligence*, 44(7):3634–3646, 2021.
- [16] J. H. Friedman. Greedy function approximation: a gradient boosting machine. *The Annals of Statistics*, 29:1189–1232, 2001.

- [17] A. Gammerman, V. Vovk, and V. Vapnik. Learning by transduction. In *Proceedings of the Annual Conference on Uncertainty in Artificial Intelligence (UAI)*, pages 148–155, Madison, Wisconsin, USA, 1998.
- [18] R. Garnett. *Bayesian Optimization*. Cambridge University Press, 2023.
- [19] A. Genz. Numerical computation of multivariate normal probabilities. *Journal of Computational and Graphical Statistics*, 1(2):141–149, 1992.
- [20] C. Guo, G. Pleiss, Y. Sun, and K. Q. Weinberger. On calibration of modern neural networks. In *Proceedings of the International Conference on Machine Learning (ICML)*, pages 1321–1330, Sydney, Australia, 2017.
- [21] J. H. Halton. On the efficiency of certain quasi-random sequences of points in evaluating multi-dimensional integrals. *Numerische Mathematik*, 2:84–90, 1960.
- [22] F. Hutter, H. H. Hoos, and K. Leyton-Brown. Sequential model-based optimization for general algorithm configuration. In *Proceedings of the International Conference on Learning and Intelligent Optimization (LION)*, pages 507–523, Rome, Italy, 2011.
- [23] T. Joachims. Transductive learning via spectral graph partitioning. In *Proceedings of the International Conference on Machine Learning (ICML)*, pages 290–297, Washington, District of Columbia, USA, 2003.
- [24] J. Kim and S. Choi. On uncertainty estimation by tree-based surrogate models in sequential model-based optimization. In *Proceedings of the International Conference on Artificial Intelligence and Statistics (AISTATS)*, pages 4359–4375, Virtual, 2022.
- [25] D. P. Kingma and J. L. Ba. Adam: A method for stochastic optimization. In *Proceedings of the International Conference on Learning Representations (ICLR)*, San Diego, California, USA, 2015.
- [26] A. Klein and F. Hutter. Tabular benchmarks for joint architecture and hyperparameter optimization. *arXiv preprint arXiv:1905.04970*, 2019.
- [27] T. Kloek and H. K. van Dijk. Bayesian estimates of equation system parameters: an application of integration by Monte Carlo. *Econometrica: Journal of the Econometric Society*, pages 1–19, 1978.
- [28] H. J. Kushner. A new method of locating the maximum point of an arbitrary multipeak curve in the presence of noise. *Journal of Basic Engineering*, 86(1):97–106, 1964.
- [29] Y. LeCun, C. Cortes, and C. J. C. Burges. The MNIST database of handwritten digits. <http://yann.lecun.com/exdb/mnist/>, 1998.
- [30] R. Martinez-Cantin, K. Tee, and M. McCourt. Practical Bayesian optimization in the presence of outliers. In *Proceedings of the International Conference on Artificial Intelligence and Statistics (AISTATS)*, pages 1722–1731, Lanzarote, Canary Islands, Spain, 2018.
- [31] J. Moćkus, V. Tiesis, and A. Žilinskas. The application of Bayesian methods for seeking the extremum. *Towards Global Optimization*, 2:117–129, 1978.
- [32] R. Müller, S. Kornblith, and G. E. Hinton. When does label smoothing help? In *Advances in Neural Information Processing Systems (NeurIPS)*, volume 32, Vancouver, British Columbia, Canada, 2019.
- [33] E. A. Nadaraya. On estimating regression. *Theory of Probability and Its Applications*, 9(1): 141–142, 1964.
- [34] J. Qin. Inferences for case-control and semiparametric two-sample density ratio models. *Biometrika*, 85(3):619–630, 1998.
- [35] C. E. Rasmussen and C. K. I. Williams. *Gaussian Processes for Machine Learning*. MIT Press, 2006.

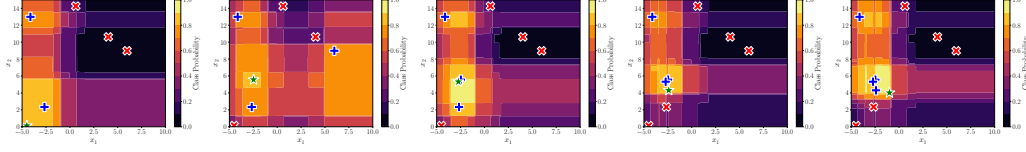
- [36] P. Rigollet. Generalization error bounds in semi-supervised classification under the cluster assumption. *Journal of Machine Learning Research*, 8(7):1369–1392, 2007.
- [37] M. Seeger. Learning with labeled and unlabeled data. Technical Report Technical Report, University of Edinburgh, 2000.
- [38] B. J. Shields, J. Stevens, J. Li, M. Parasram, F. Damani, J. I. M. Alvarado, J. M. Janey, R. P. Adams, and A. G. Doyle. Bayesian reaction optimization as a tool for chemical synthesis. *Nature*, 590(7844):89–96, 2021.
- [39] A. Singh, R. D. Nowak, and X. Zhu. Unlabeled data: now it helps, now it doesn’t. In *Advances in Neural Information Processing Systems (NeurIPS)*, volume 21, pages 1513–1520, Vancouver, British Columbia, Canada, 2008.
- [40] J. Snoek, H. Larochelle, and R. P. Adams. Practical Bayesian optimization of machine learning algorithms. In *Advances in Neural Information Processing Systems (NeurIPS)*, volume 25, pages 2951–2959, Lake Tahoe, Nevada, USA, 2012.
- [41] I. M. Sobol’. On the distribution of points in a cube and the approximate evaluation of integrals. *Zhurnal Vychislitel’noi Matematiki i Matematicheskoi Fiziki*, 7(4):784–802, 1967.
- [42] J. Song, L. Yu, W. Neiswanger, and S. Ermon. A general recipe for likelihood-free Bayesian optimization. In *Proceedings of the International Conference on Machine Learning (ICML)*, pages 20384–20404, Baltimore, Maryland, USA, 2022.
- [43] J. T. Springenberg, A. Klein, S. Falkner, and F. Hutter. Bayesian optimization with robust Bayesian neural networks. In *Advances in Neural Information Processing Systems (NeurIPS)*, volume 29, pages 4134–4142, Barcelona, Spain, 2016.
- [44] N. Srinivas, A. Krause, S. Kakade, and M. Seeger. Gaussian process optimization in the bandit setting: No regret and experimental design. In *Proceedings of the International Conference on Machine Learning (ICML)*, pages 1015–1022, Haifa, Israel, 2010.
- [45] M. Sugiyama, T. Suzuki, and T. Kanamori. *Density ratio estimation in machine learning*. Cambridge University Press, 2012.
- [46] L. C. Tiao, A. Klein, M. Seeger, E. V. Bonilla, C. Archambeau, and F. Ramos. BORE: Bayesian optimization by density-ratio estimation. In *Proceedings of the International Conference on Machine Learning (ICML)*, pages 10289–10300, Virtual, 2021.
- [47] G. S. Watson. Smooth regression analysis. *Sankhyā: The Indian Journal of Statistics, Series A*, 26:359–372, 1964.
- [48] C. Wei, K. Shen, Y. Chen, and T. Ma. Theoretical analysis of self-training with deep networks on unlabeled data. In *Proceedings of the International Conference on Learning Representations (ICLR)*, Virtual, 2020.
- [49] M. Yamada, T. Suzuki, T. Kanamori, H. Hachiya, and M. Sugiyama. Relative density-ratio estimation for robust distribution comparison. In *Advances in Neural Information Processing Systems (NeurIPS)*, volume 24, pages 594–602, Granada, Spain, 2011.
- [50] S. Zhang, M. Wang, S. Liu, P.-Y. Chen, and J. Xiong. How does unlabeled data improve generalization in self-training? a one-hidden-layer theoretical analysis. In *Proceedings of the International Conference on Learning Representations (ICLR)*, Virtual, 2022.
- [51] D. Zhou, O. Bousquet, T. N. Lal, J. Weston, and B. Schölkopf. Learning with local and global consistency. In *Advances in Neural Information Processing Systems (NeurIPS)*, volume 16, pages 321–328, Vancouver, British Columbia, Canada, 2003.
- [52] X. Zhu. Semi-supervised learning literature survey. Technical Report Computer Sciences TR-1530, University of Wisconsin–Madison, 2005.
- [53] X. Zhu and Z. Ghahramani. Learning from labeled and unlabeled data with label propagation. Technical Report CMU-CALD-02-107, Carnegie Mellon University, 2002.

## Supplementary Material

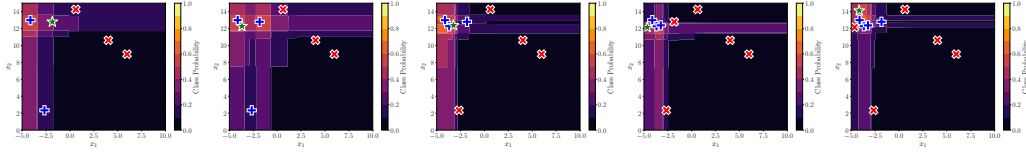
In this document, we cover the contents that are missed in the main article.

### S.1 Additional Comparisons of BORE and LFBO

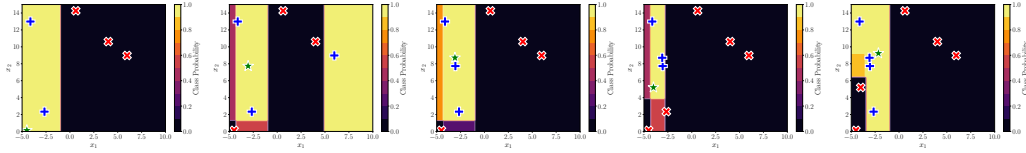
In addition to Figure 1, we include additional comparisons of BORE and LFBO by random forests [8], gradient boosting [16], and XGBoost [13] for the Branin function. For Figures 1, s.1, and s.2, we use  $\zeta = 0.33$  and  $\beta = 0.5$ .



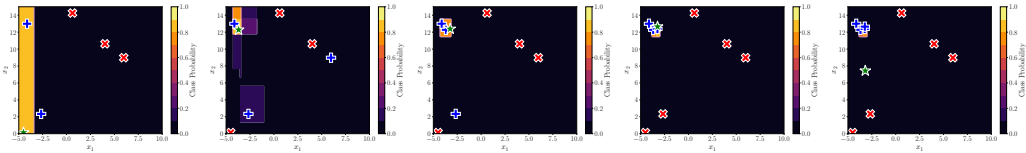
(a) Random forests, BORE, Iterations 1 to 5



(b) Random forests, LFBO, Iterations 1 to 5



(c) Gradient boosting, BORE, Iterations 1 to 5



(d) Gradient boosting, LFBO, Iterations 1 to 5

Figure s.1: Comparisons of BORE and LFBO by random forests and gradient boosting for the Branin function. It follows the configurations described in Figure 1.

### S.2 Details of DRE-BO-SSL

Algorithm s.1 describes a procedure to label unlabeled data points; see the main article for the details of DRE-BO-SSL.

### S.3 Experiment Details

Here we present the missing details of the experiments shown in the main part.

To carry out the experiments in our work, we use dozens of commercial Intel and AMD CPUs. For the experiments on minimum multi-digit MNIST search, the NVIDIA GeForce RTX 3090 GPU is used.

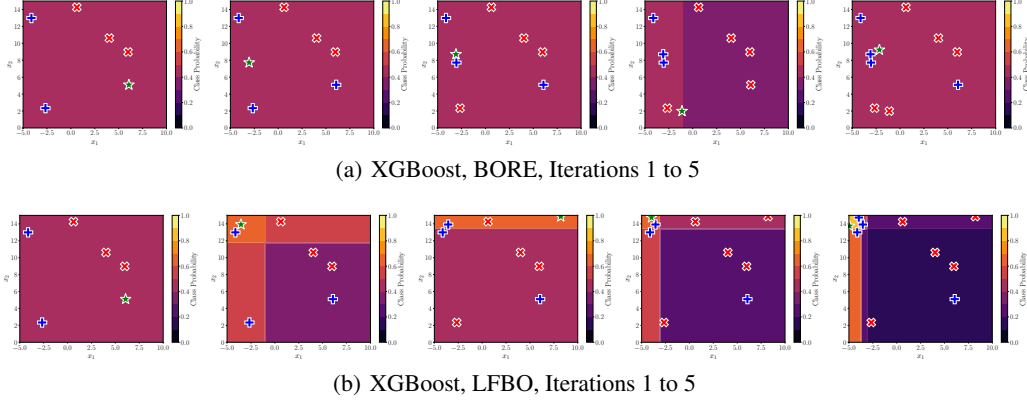


Figure s.2: Comparisons of BORE and LFBO by XGBoost for the Branin function. It follows the configurations described in Figure 1.

---

#### Algorithm s.1 Labeling Unlabeled Data

---

**Input:** Labeled data points  $\mathbf{X}_l$ , their labels  $\mathbf{C}_l$ , unlabeled data points  $\mathbf{X}_u$ , maximum iterations  $\tau$ , and a tolerance  $\varepsilon$ . Additionally, a clamping factor  $\alpha$  for label spreading.

**Output:** Propagated labels  $\hat{\mathbf{C}}$ .

- 1: Initialize propagated labels  $\hat{\mathbf{C}}$  of  $\mathbf{X}$ .
  - 2: Compute similarities  $\mathbf{W}$  and a degree matrix  $\mathbf{D}$ .
  - 3: Compute transition probabilities  $\mathbf{P}$  with  $\mathbf{W}$  and  $\mathbf{D}$ .
  - 4: **repeat**
  - 5:   Propagate  $\hat{\mathbf{C}}$  with  $\mathbf{P}$  and the previous  $\hat{\mathbf{C}}$ , and additionally  $\alpha$  for label spreading.
  - 6:   Normalize  $\hat{\mathbf{C}}$  row-wise.
  - 7: **until** a change of  $\hat{\mathbf{C}}$  converging to  $\varepsilon$  or reaching  $\tau$ .
- 

#### S.3.1 Details of Baseline Methods

As the competitors of our method, we test the following baseline methods:

- Gaussian process, EI and UCB: It is a Bayesian optimization strategy, which is defined with Gaussian process regression with the Matérn 5/2 kernel [35]. Expected improvement [31] and GP-UCB [44] are used as acquisition functions.
- Random forest, BORE and LFBO: These are BORE and LFBO with random forests [8] with 1000 decision trees. Min. samples to split are set to 2.
- Gradient boosting, BORE and LFBO: These methods are BORE and LFBO with gradient boosting classifiers [16] with 100 decision trees. Learning rate for the classifier is set to 0.3.
- XGBoost, BORE and LFBO: Similar to gradient boosting, BORE and LFBO with XGBoost have 100 decision trees as base learners with learning rate 0.3.
- MLP, BORE and LFBO: These methods are built with two-layer fully-connected networks. The detail of the multi-layer perceptron is described as follows.

The architecture of a multi-layer perceptron is

First layer: fully-connected, input dimensionality  $d$ , output dimensionality 32, ReLU;

Second layer: fully-connected, input dimensionality 32, output dimensionality 1, Logistic,

where  $d$  is the dimensionality of the problem we solve.

Note that configurations for the baseline methods follow the configurations described in the work [42].

Table s.1: Search space for Tabular Benchmarks.

Hyperparameter	Possible Values
The number of units for 1st layer	{16, 32, 64, 128, 256, 512}
The number of units for 2nd layer	{16, 32, 64, 128, 256, 512}
Dropout rate for 1st layer	{0.0, 0.3, 0.6}
Dropout rate for 2nd layer	{0.0, 0.3, 0.6}
Activation function for 1st layer	{“tanh”, “relu”}
Activation function for 2nd layer	{“tanh”, “relu”}
Initial learning rate	$\{5 \times 10^{-4}, 1 \times 10^{-3}, 5 \times 10^{-3}, 1 \times 10^{-2}, 5 \times 10^{-2}, 1 \times 10^{-1}\}$
Learning rate scheduling	{“cosine”, “constant”}
Batch size	{8, 16, 32, 64}

### S.3.2 Details of Tabular Benchmarks

The search space of Tabular Benchmarks [26] is described in Table s.1.

### S.3.3 Details of NATS-Bench



Figure s.3: Neural network architecture in NATS-Bench. Orange blocks are optimized.

Table s.2: Search space for NATS-Bench.

Hyperparameter	Possible Values
Output channels of 1st convolutional layer	{8, 16, 24, 32, 40, 48, 56, 64}
Output channels of 1st cell stage	{8, 16, 24, 32, 40, 48, 56, 64}
Output channels of 1st residual block	{8, 16, 24, 32, 40, 48, 56, 64}
Output channels of 2nd cell stage	{8, 16, 24, 32, 40, 48, 56, 64}
Output channels of 2nd residual block	{8, 16, 24, 32, 40, 48, 56, 64}

We describe the search space for NATS-Bench [15] in Figure s.3 and Table s.2.

### S.3.4 Details of Minimum Multi-Digit MNIST Search.

Since multi-digit MNIST, which is composed of images of size (28, 84), is high-dimensional, some of the methods used in this work, e.g., methods with random forests, gradient boosting, and XGBoost, struggle to process such data. Therefore, we embed an original image to a lower-dimensional vector using an auxiliary convolutional neural network. The convolutional neural network is trained to classify a three-digit image to one of labels from “000” to “999”, with the following architecture:

First layer: convolutional, input channel 1, output channel 8, kernel size  $3 \times 3$ , padding 1, ReLU, max-pooling  $2 \times 2$ ;

Second layer: convolutional, input channel 8, output channel 16, kernel size  $3 \times 3$ , padding 1, ReLU, max-pooling  $2 \times 2$ ;

Third layer: convolutional, input channel 16, output channel 32, kernel size  $3 \times 3$ , padding 1, ReLU, max-pooling  $2 \times 2$ ;

Fourth layer: fully-connected, input dimensionality 960, output dimensionality 128, ReLU;

Fifth layer: fully-connected, input dimensionality 128, output dimensionality 64, ReLU;

Sixth layer: fully-connected, input dimensionality 64, output dimensionality 1000, Softmax.

The Adam optimizer [25] with learning rate  $1 \times 10^{-3}$  is used to train the network for 100 epochs. To train and test the model fairly, we create a training dataset of 440,000 three-digit images, a validation

dataset of 40,000 three-digit images, and a test dataset of 80,000 three-digit images using a training dataset of 55,000 single-digit images, a validation dataset of 5,000 single-digit images, and a test dataset of 10,000 single-digit images in the original MNIST dataset [29]. In addition, an early stopping technique is utilized by comparing the current validation loss to the average of validation losses for the recent five epochs. Eventually, our network achieves 99.6% in the training dataset, 97.0% in the validation dataset, and 96.9% in the test dataset.

To construct a fixed-size pool, we use 80,000 embeddings of dimensionality 64, which are derived from the outputs of the fifth layer without ReLU, by passing the test dataset of three-digit images through the network.

## S.4 Discussion on Free Parameters in Label Propagation and Label Spreading

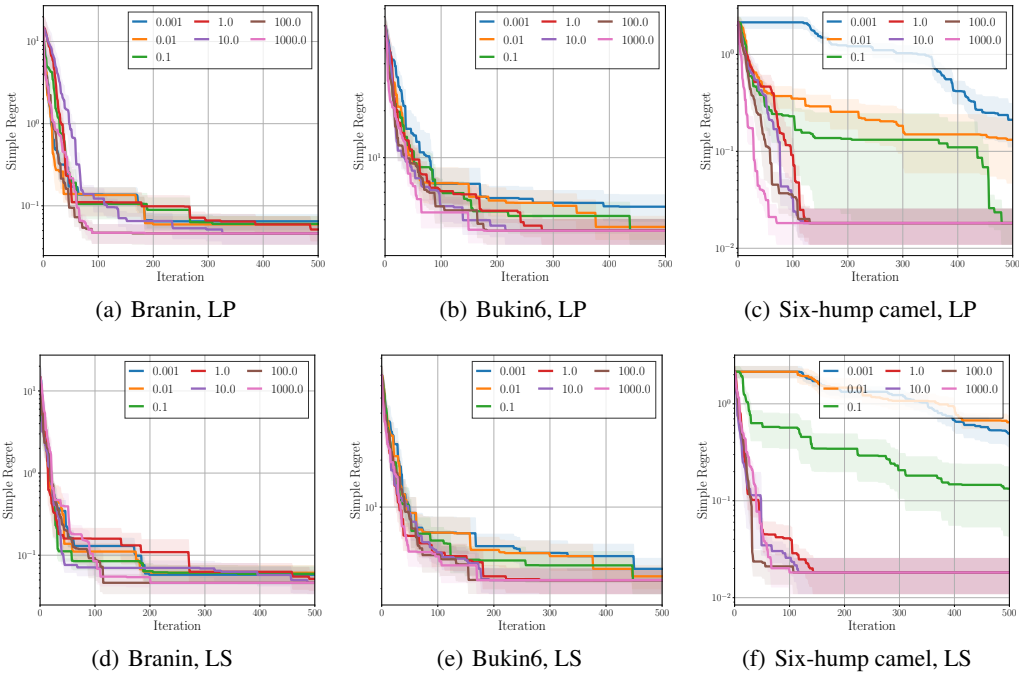


Figure S.4: Effects of free parameters in label propagation, denoted as LP, and label spreading, denoted as LS. All experiments are repeated 10 times.

As shown in Figure S.4, we empirically analyze the effects of a free parameter  $\beta$  in label propagation and label spreading. For the cases of three benchmark functions, higher  $\beta$  tends to show better performance than lower  $\beta$ . More precisely, the cases with  $\beta = 100$  and  $\beta = 1000$  perform well, while the cases with  $\beta = 0.001$  and  $\beta = 0.01$  show inferior performance.

## S.5 Discussion on Unlabeled Point Sampling

We design two scenarios to analyze the effects of the number of unlabeled points  $n_u$  and sampling strategies in a process of unlabeled point sampling, where unlabeled points are not provided.

For the first scenario, we conduct five settings, no unlabeled data, which implies that transductive learning is not used, and  $n_u = 10, 100, 1000, 10000$ . Interestingly, no unlabeled data underperforms the settings with unlabeled data as in Figure S.5. However, the effects of the number of unlabeled points are unclear. We consider that  $\gamma$  is different across benchmarks and iterations and it makes optimization results sensitive to  $n_u$ .



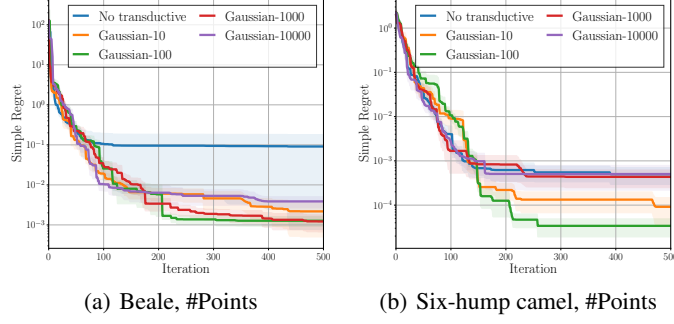


Figure s.5: Effects of the number of unlabeled points for unlabeled point sampling. For these experiments, label spreading is used as a semi-supervised classifier. Similar to other experiments, all experiments are repeated 10 times.

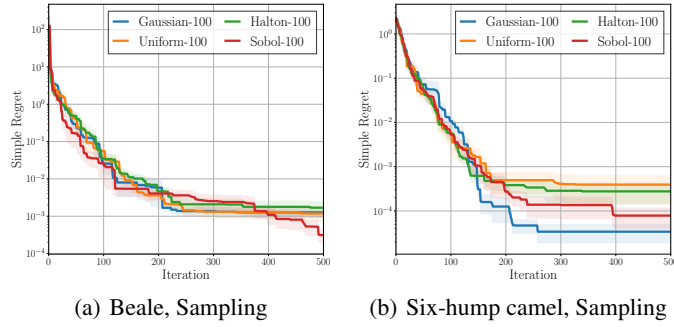


Figure s.6: Effects of sampling strategies for unlabeled point sampling. For these experiments, label spreading is used as a semi-supervised classifier. Similar to other experiments, all experiments are repeated 10 times.

As another scenario, we test the effects of sampling strategies. Four strategies, the truncated multi-variate normal distributions, uniform distributions, Halton sequences [21], and Sobol' sequences [41], are compared. As presented in Figure s.6, the normal distribution tends to be better than the other sampling methods, but it is not always the best. Similar to the previous scenario on the effects of  $n_u$ , we presume that it is affected by  $\gamma$ , which is hard to define in practice.

## S.6 Discussion on Pool Sampling

To see the impact of an additional hyperparameter, i.e., the size of a subset of the original pool, which is introduced to speed up semi-supervised learning algorithms, we demonstrate numerical analyses on pool sampling. As presented in Figure s.7, our framework tends not to be sensitive for a subset size. Thus, we can conclude that this subsampling technique can be used in our method without significant performance loss.

## S.7 Broader Impacts

Our work does not have a direct negative societal impact because it proposes a new Bayesian optimization method to optimize a black-box function. However, in the sense of optimization, this line of research can be used in optimizing any objective functions including harmful and unethical optimization tasks.

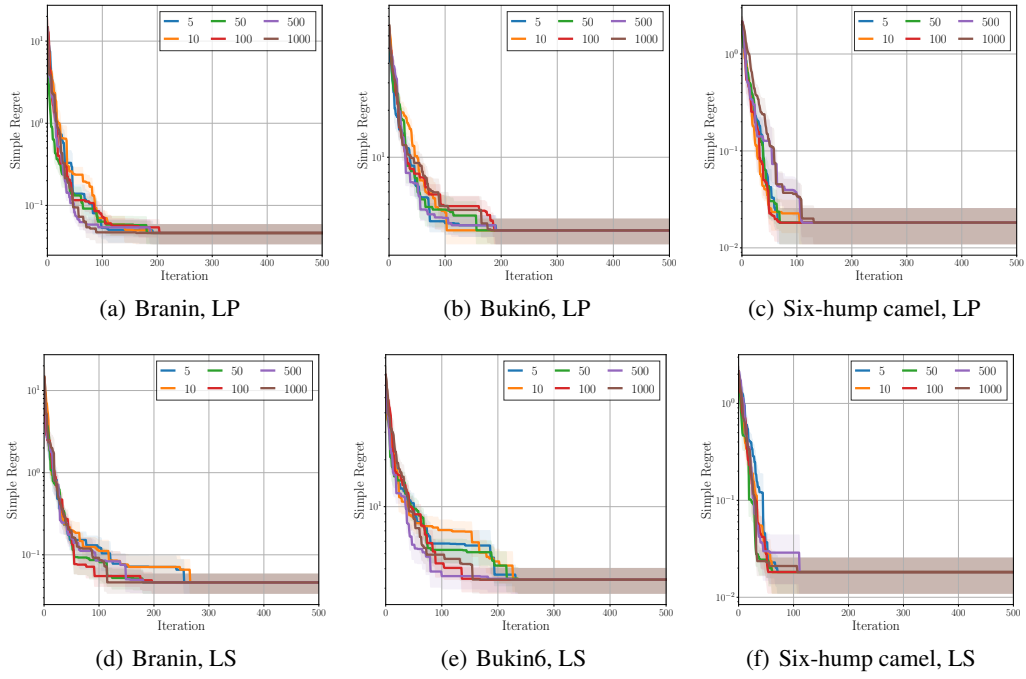


Figure s.7: Effects of pool sampling for a case with fixed-size pools. All experiments are repeated 10 times, and LP and LS stand for label propagation and label spreading, respectively.